JOURNAL OF APPLIED POLYMER SCIENCE VOL. 17, PP. 3069–3083 (1973)

A Rotating Sphere Viscometer

J. V. KELKAR, R. A. MASHELKAR, and J. ULBRECHT, *Dept. of Chemical Engineering, University of Salford, Salford M5 4WT, England*

Synopsis

The use of a rotating sphere viscometer for the measurement of parameters in the flow curves of inelastic as well as viscoelastic liquids is examined. An experimental investigation of the primary flow around a sphere rotating in Newtonian and viscoelastic liquids is carried out by using a new "three-dimensional particle technique." Currently available theoretical analyses of rotation of a sphere in viscoelastic liquids are shown to be inadequate to describe the experimental primary velocity distribution data. Theoretical results for the primary distribution derived on the basis of a creeping flow of a power law liquid are found to describe the experimental data well. This distribution is then used to derive torque–angular velocity relationships, which are then confirmed experimentally for both inelastic and viscoelastic liquids. The results of this work justify the use of a rotating sphere viscometer as a useful tool for the measurement of parameters of flow curves of inelastic and viscoelastic liquids.

INTRODUCTION

The usual techniques for the measurement of rheological properties of polymer solutions and melts make use of the simple viscometric flow arrangements (e.g., capillary flow, couette flow, cone-and-plate flow, etc.). Although the kinematics of the flows involved in such viscometric arrangements is quite simple (a simple shear flow), to satisfy the conditions of such flows is sometimes experimentally difficult. For instance, the entrance effects in the capillary flow have to be accurately accounted for. In the case of the cone-and-plate flow, the apex angle of the cone has to be machined precisely to a very small value so as to satisfy the conditions of simple shear flow as closely as possible. The problem of accounting for inertial effects can be significant for all the rotational viscometric flows. Problems of nonisothermality due to the temperature rise as a result of viscous dissipation are also unavoidable in very small gaps. Finally, the stability considerations of flow may also cause difficulties in some cases.

It is interesting to think of other simple experimental techniques which can be used for a meaningful measurement of the rheological properties. One such arrangement is the "rotational sphere viscometer." This essentially consists of a spherical body which rotates around its own axis and is placed centrally in the test fluid. This experimental arrangement is fairly simple and cheap. It does not require more than a sensitive dynamometer and a provision for keeping a constant temperature of the sample liquid.

In a previous paper[1] we have examined the rotating sphere viscometer (referred to as RSV hereafter) as a tool for the determination of zero-shear viscosity of inelastic as well as viscoelastic liquids. In this paper, we propose a procedure for the determination of parameters of a flow curve, which again will be applicable to both inelastic as well as viscoelastic liquids.

ANALYSIS OF THE PROBLEM AND PREVIOUS WORK

Nonviscometric flows around various types of rotating bodies have been used extensively in polymer, food, and other processing industries. Without any exact hydrodynamic analysis, they can offer point value of apparent viscosities if adequately calibrated by Newtonian liquids. Two nonviscometric rotational flows, however, have been analyzed in the past in order to obtain rational expressions for shear rate and shear stress from the calculated velocity profiles and to make use of such nonviscometric flows for viscometric purposes. These flows are: the flow around a rotating disc and also a rotating sphere.

A rotating disc viscometer was proposed by Wichterle and Ulbrecht[2] for inelastic non-Newtonian liquids. The procedure is based upon the analysis of boundary layer flow of Ostwald-de Waele (power law) liquids in the vicinity of the rotating disc. From the torque–angular velocity data the values of the flow index n and the consistency k can be directly determined. Since a true creeping flow regime around a disc rotating in an unbounded liquid cannot be physically materialized, the method is confined to the high-Reynolds-number laminar boundary layer flow regime. For viscous polymer solutions and melts it is difficult to approach this regime experimentally, and hence the method is applicable to rather dilute solutions. Kale et al.[3] have, in addition, shown experimentally that the method cannot be used for viscoelastic liquids because the torque in the laminar boundary layer regime of flow is considerably reduced on account of the presence of elasticity.

The method discussed above had ignored elasticity but made use of a realistic model for the shear-thinning behavior. However, in the case of the work done so far using a rotating sphere, the analysis is based upon a second-order or a third-order approximation of a "simple memory fluid." This model accounts for the presence of elasticity but relies upon an unrealistic interpretation of flow curves. Mashelkar et al.[1] have critically analyzed the previous work in this category done by Giesekus,[4] Walters and Savins,[5] and Hermes[6] and have also shown that the viscosity function resulting from third-order approximation cannot be fitted to the actual flow curves for polymer solutions.

The aim of this work is to devise an evaluation procedure for a rotating body viscometer under nonsimple shear flow conditions, which would use the power law type of interpretation of the flow curve and simultaneously to analyze the extent to which elastic and other second-order effects affect both the primary velocity distribution as well as the torque–angular ve-

locity curves. A rotating sphere has been chosen for this matter because of its simplicity.

THEORETICAL

As pointed out earlier, in the conventional viscometric arrangements the kinematics of the flow are simple in the sense that there is only one non-vanishing velocity component depending on only one coordinate direction. Hence, defining the velocity distribution and calculating shear rate and shear stress distribution and eventually the torque (or the pressure drop) is a straightforward problem. Unfortunately, this problem is quite difficult in the case of RSV. In the following, we briefly summarize and simultaneously analyze the situations which arise as the rotational speed of the sphere as well as the rheological complexities of the fluids increase.

Consider that the radius of the sphere is a and that it rotates steadily with the angular velocity Ω about a vertical diameter, the liquid extending to infinity in all directions. We refer all the quantities concerning the liquid to spherical polar coordinates (r, θ, ϕ), r being measured from the center of the sphere and $\theta = 0$ representing the axis of rotation; v_r, v_θ, and v_ϕ are the respective velocity components of the velocity vector v.

Consider a Newtonian liquid of density ρ and viscosity η_0 in which a sphere is rotating at low Reynolds number ($Re \ll 1$). There is no secondary flow and hence $v_r = v_\theta = 0$. This problem is simply solved,[7] and the primary or rotational flow distribution is

$$v_\phi = \frac{\Omega a^3 \sin\theta}{r^2} \tag{1}$$

and the torque on the sphere T is calculated as

$$T = 8\pi a^3 \Omega \eta_0. \tag{2}$$

At higher Reynolds numbers ($Re > 1$), the secondary flow effects come into picture. The fluid is drawn toward the sphere along the axis of rotation and is thrown away along the equator because of the centrifugal forces. In this case, v_r, v_θ, and v_ϕ are all finite and the solution of the equation of motion is more difficult. The velocity distribution is now given[8] as

$$v_r = \frac{\rho\Omega^2 a^5}{8\eta_0 r^2}(1 - a/r)^2(3\sin^2\theta - 2) \tag{3}$$

$$v_\theta = \frac{\rho\Omega^2 a^6}{4\eta_0 r^3}(1 - a/r)\sin\theta\cos\theta \tag{4}$$

$$v_\phi = \frac{\Omega a^3 \sin\theta}{r^2} + \frac{\rho^2\Omega^2 a^4}{\eta_0^2}\left[H_1 \sin\theta + H_3\left(\sin^3\theta - \frac{4}{5}\sin\theta\right)\right] \tag{5}$$

where

$$H_1 = -\frac{(a/r)^5}{120} + \frac{(a/r)^4}{50} - \frac{(a/r)^3}{80} + \frac{(a/r)^2}{1200} \tag{6}$$

and

$$H_3 = \frac{(a/r)^5}{64} + \frac{(a/r)^3}{16} + \left(\frac{\log (a/r)}{28}\right) - \frac{5}{64}\left(\frac{a}{r}\right)^4. \tag{7}$$

The torque on the sphere is calculated as

$$T = 8\pi a^3 \Omega \eta_0 + \frac{\pi}{150} \Omega^3 a^7 \rho^2 \eta_0. \tag{8}$$

The problem of the solution of equation of motion for non-Newtonian liquids presents considerably more difficulties. For the most general case of a viscoelastic liquid, there are many anomalies observed under different flow conditions. In the simplest case of a simple shear flow, such a liquid exhibits a shear thinning viscosity and also normal stresses. Several constitutive equations expressed in properly invariant forms[9] are able to show these peculiarities at least qualitatively. However, even when the form of stress predicted by even the simplest of such constitutive equations is substituted in the equation of motion, we have quite a complicated situation due to the nonlinear constitutive relationships portraying the rheological complexities of the viscoelastic liquids as well as the nonlinear inertial terms.

An alternative is usually found by using a relatively simple constitutive equation (such as a third-order approximation) and using approximate mathematical techniques (such as perturbation analysis). In the particular case of a rotating sphere, the information derived by this procedure is only qualitative, in that it can help us in showing that the rotation of sphere can produce some strange flow patterns. Such velocity distributions, however, cannot be used for an exact quantitative assessment of the torque on the sphere because, for example, the approximation of a third-order fluid is valid only in the asymptotic region of vanishingly small deformation rates and as such is far from satisfied in practical situations. When using approximations of higher orders, the problem of determining the torque exerted on the surface of the sphere becomes mathematically untractable, apart from the fact that the number of adjustable parameters becomes impracticably large. However, reasonable assumptions can be made for the evaluation of the torque if one critically analyses the primary and secondary flows.

The mathematical expression for the torque exerted on the sphere is given by integrating the shear stress $\tau_{r\phi}$ on the surface of the sphere and multiplying the resulting force by the lever arm. Thus, the expression for the torque is

$$T = \int_0^\pi \tau_{r\phi}\Big|_{r=a} 2\pi a^3 \sin^2\theta \, d\theta. \tag{9}$$

The expression for $\tau_{r\phi}$ is dependent only on the space derivatives of v_ϕ (the primary flow) in the spherical coordinate system. Thus, for instance, in the case of a Newtonian liquid,

$$\tau_{r\phi} = \eta_0 \left[-r \frac{\partial}{\partial r} \left(\frac{v_\phi}{r} \right) \right]. \tag{10}$$

This means that only the extent of modification of the primary flow, v_ϕ, particularly in the vicinity of the sphere, contributes to the changes in the magnitude of the torque. If one now examines the expressions for v_ϕ in the case of a Newtonian liquid, one finds that the presence of secondary velocity has not really substantially contributed to the primary flow, and it could still be well approximated by the expression valid in the creeping flow regime, eq. (1), particularly very near the sphere. This indicates that up to a certain limit the torque is not substantially affected by the presence of such inertial effects. More quantitatively, if one rewrites eq. (8) as

$$C_M = 8\pi \left(\frac{1}{Re} + \frac{Re}{600} \right) \tag{11}$$

where C_M = power number = $T/\rho a^5 \Omega^2$, then it is seen that even at $Re = 5$, the contribution to the torque on the sphere is only about 4.25%. If we now examine the expression for v_ϕ in the case of a viscoelastic liquid,[8] once again it is clearly seen that the combined influence of inertia and elasticity does not affect v_ϕ and consequently the torque in a substantial way. This observation has some importance because it tells us that a good approximation to v_ϕ could be found by approximating it by the expression under creeping flow conditions. The problem of solution of the equation of motion under creeping flow conditions is rather simple. The equation of motion in the ϕ direction of the spherical coordinate system is given as

$$\frac{\partial \tau_{r\phi}}{\partial r} + 3 \frac{\tau_{r\phi}}{r} = 0. \tag{12}$$

The above equation has to be solved with the B.C.

$$v_\phi = a\Omega \sin \theta \qquad \text{at } r = a \tag{13}$$

and

$$v_\phi = 0 \qquad \text{as } r \to \infty. \tag{14}$$

If we assume that the flow behaviour of the liquid is well represented by a power law model, then we have

$$\tau_{r\phi} = -K \left| r \frac{\partial}{\partial r} \left(\frac{v_\phi}{r} \right) \right|^{n-1} r \frac{\partial}{\partial r} \left(\frac{v_\phi}{r} \right). \tag{15}$$

Substituting eq. (15) in (12) and solving, we get an expression for v_ϕ as

$$\frac{v_\phi}{r\Omega \sin \theta} = \left(\frac{a}{r} \right)^{3/n}. \tag{16}$$

Substituting eq. (16) back in (15) gives the shear stress distribution as

$$\tau_{r\phi} = K \left(\frac{a}{r} \right)^3 \left(\frac{3\Omega \sin \theta}{n} \right)^n. \tag{17}$$

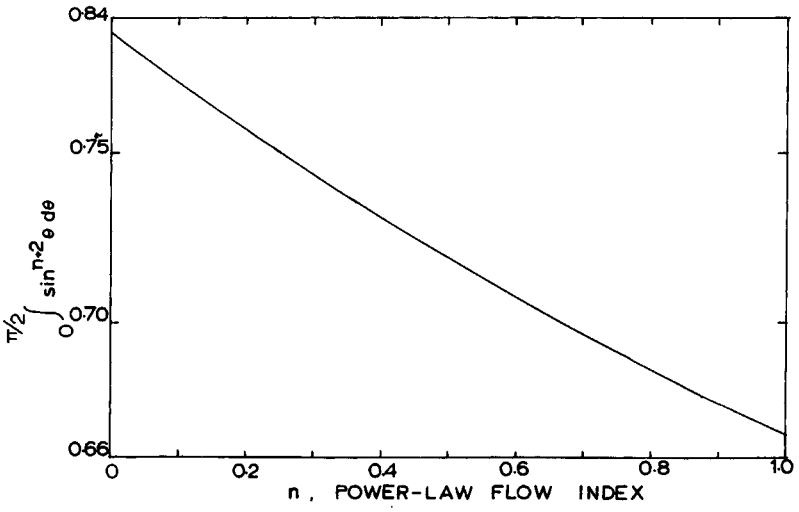

Fig. 1. The integral in eq. (18) plotted as a function of n.

Substituting this expression for $\tau_{r\phi}$ in eq. (9) and integrating, the torque on the sphere is obtained as

$$T = 4\pi a^3 K \left(\frac{3\Omega}{n}\right)^n \int_0^{\pi/2} (\sin\theta)^{2+n}\, d\theta. \tag{18}$$

The integral has to be evaluated numerically. A graph of the value of the integral as a function of the flow behavior index n is given in Figure 1.

The validity of such a simple approximation for v_ϕ as well as the torque on the sphere could only be tested experimentally by measuring both the velocity distribution as well as the torque exerted on the sphere in different liquids.

EXPERIMENTAL

Four different spheres (radii from 0.635 to 2.64 cm) were used for the purpose of experimental work. Billiard balls were found to be quite suitable for this purpose. Most of the work was done in a 30-cm-diam. cylindrical vessel. In the case of the determination of velocity distribution, a square vessel of dimensions 34 cm × 34 cm was used. This avoided the difficulties due to optical distortion. The liquids used were an aqueous solution of sodium salt of carboxy methyl cellulose (CMC) (Edifas B ICI), aqueous solutions of polyacrylamide (PAA) (Separan AP30, Dow Chemicals), and a mixture of an aqueous solution of PAA and hydroxyethyl cellulose (HEC).

All the work was performed in a constant-temperature room at a temperature of 20° ± 1°C. The flow curves and normal stress data were obtained on a Weissenberg rheogoniometer (Model R18) at the same temperature at which the rotational sphere experiments were conducted.

Measurement of Torque

An indigenously manufactured flexible drive shaft dynamometer was used for the measurement of torques. The details of this dynamometer are given by Mashelkar et al.[1] and Kelkar.[10]

Measurement of Velocity Distribution

Different techniques of measurement of velocity distribution have been used in the past by different workers. Kelkar[10] has summarized these methods and clearly pointed out the respective advantages and disadvantages.

In this work, we have used a new optical technique, which may be called a "three-dimensional particle technique." The principle of the technique is to make the suspended neutrally buoyant particles follow the fluid motion and track their motion in mutually perpendicular directions by using two cameras. If the work is carried out in dark surroundings, then a bright light source flashing at specific predetermined time intervals allows one to establish the motion of the particles in the form of multiple-exposure photographs from the two directions. From each of these photographs one can specify the position of the particle in space with respect to a fixed frame of reference in any coordinate system and at different intervals of time. The differentiation of these position–time data yields the information about the instantaneous velocity as well as the velocity distribution. This technique has many advantages; in particular, one is in a position to trace not only the paths of the particles but also the exact magnitude of all the velocity components.

Two large electronic strobe units were fixed along the side of a square perspex vessel (34 cm $\times$ 34 cm) which contained the test fluid. The length of each flash was 5×10^{-3} sec. The interval between each flash could be controlled by a constant frequency generator. The vessel was placed on a transparent platform and underneath it was placed at inclined-front silvered mirror. Two cameras (35-mm single-lens reflex type fitted with a telephoto lens of 135 mm focal length) were placed in such a way that each was approximately 8 feet optical distance away from the rotating body. High-density polystyrene and polyethylene particles painted with a polyurethane emulsion were used as tracer particles. Painting the particles helped in adjusting the density of the particles equal to that of the medium in which they were suspended. This also helped in improving the reflected light and this made the particles more tractable.

During an experimental run, the particles were placed in the test fluid below the equator of the sphere. The sphere was set in motion and its speed was adjusted to a predetermined value. The whole room was now made dark and the shutters of the cameras now opened. The strobes were made to flash five to fifteen times at the right frequency. This procedure recorded on the photographic film the position of the tracer particles at the instant of each flash. The film was developed in Ilford Microphane

developer to get fine-grain and high-resolution photographs. An X-Y analyzer was used to measure accurately the position of the particles w.r.t. the center of the sphere. The photographs from the two mutually perpendicular directions were combined to give the rectangular coordinates (X, Y, and Z) of the particle. These were then converted to the spherical coordinates (r, θ, ϕ) by using the well-known conversions.[11] The primary flow field was then found by differentiating the data as,

$$v_\phi = r\frac{\partial\phi}{\partial t} \simeq r\frac{\Delta\phi}{\Delta t}. \tag{19}$$

Sufficiently small increments ($\Delta\phi$ and Δt) ensured that the approximation implied in eq. (19) was followed closely. For any further details reference 10 may be consulted.

The work on velocity distribution was done with a single sphere of radius 2.64 cm rotating at 50 and 200 rpm in a Newtonian fluid (glycerine) and a viscoelastic fluid (PAA–HEC mixture). The latter was specially used for this work since it gave much better transparency than only an aqueous PAA solution.

RESULTS AND DISCUSSION

We will first examine the problem of velocity distribution. In the case of the glycerine solution at both 50 rpm (Re = 2.6) and 200 rpm (Re = 10.4), strong secondary velocities were observed and the pattern of flow was qualitatively the same as described earlier. For a quantitative comparison of the experimental primary velocity distribution, we use eq. (1) to check the deviation from the distribution predicted by creeping flow. Equation (1) may be rewritten as

$$\frac{v_\phi}{r\sin\theta} = \Omega a^3 r^{-3}. \tag{20}$$

Thus plotting $v_\phi/(r\sin\theta)$ versus r on a log–log scale should give a line of slope -3, and the line should also satisfy the boundary condition $v_\phi = r\Omega\sin\theta$ when $r = a$. Such plots based on eq. (20) are made at both the rotational speeds and are given in Figures 2 and 3. The figures show that up to $r/a = 4$, the primary flow was well described by the theoretical expression (20) even though there was a strong secondary flow present. At $r/a > 4$, there is some divergence and this could be attributed partially to the influence of the walls. The theoretical expression is calculated based on the assumption that the fluid extends to infinity. Hence, near the wall this expression appears to fail.

It is important now to consider the contribution to the torque on the sphere because of velocity gradients at different positions in the fluid. The expression for shear stress distribution for a Newtonian fluid is given by

$$\tau_{r\phi} = \eta_0\left(\frac{a}{r}\right)^3(3\Omega\sin\theta). \tag{21}$$

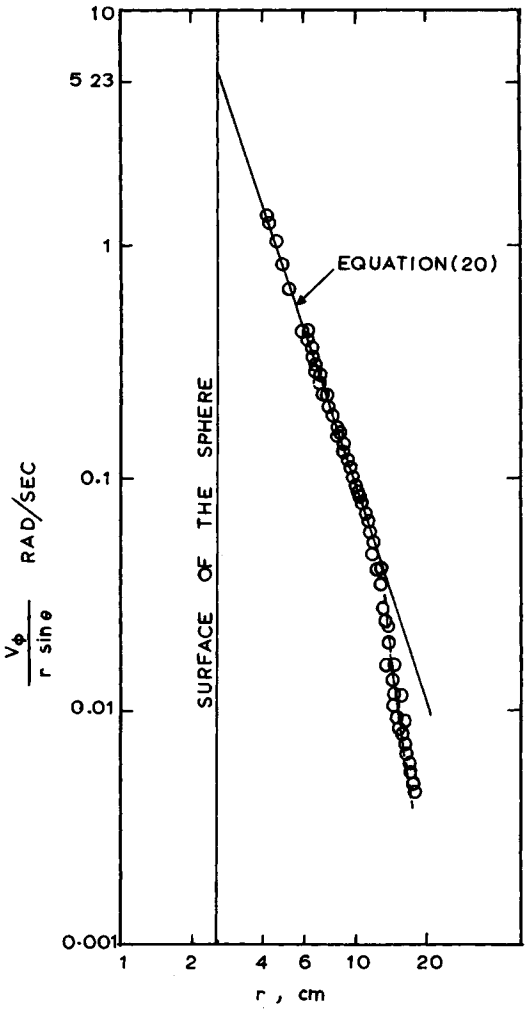

Fig. 2. Primary velocity distribution for a sphere rotating in a Newtonian glycerol solution compared with the theoretical result (rpm = 50).

It is seen that the contribution of the shear stress to the overall torque on the sphere reduces considerably as one approaches larger radial distances. Thus, at $r/a = 4$, the contribution is only $^1/_{64}$th of that at $r/a = 1$, and even smaller at further radial distances. This indicates that the presence of finite walls in a practical viscometer is unlikely to contribute significantly to the measurement of torque, and consequently it is unlikely to cause a significant error in the measurement of rheological parameters.

We now examine the primary velocity distribution in the viscoelastic liquid. The shear stress–shear rate and the primary normal stress difference–shear rate data for this fluid were obtained on the Weissenberg rheogoniometer. The solution showed a strong shear-thinning viscosity. A power law was fitted to the flow curve, and the resulting parameters were $K = 74.8$ and $n = 0.454$. The solution showed strong normal stress differ-

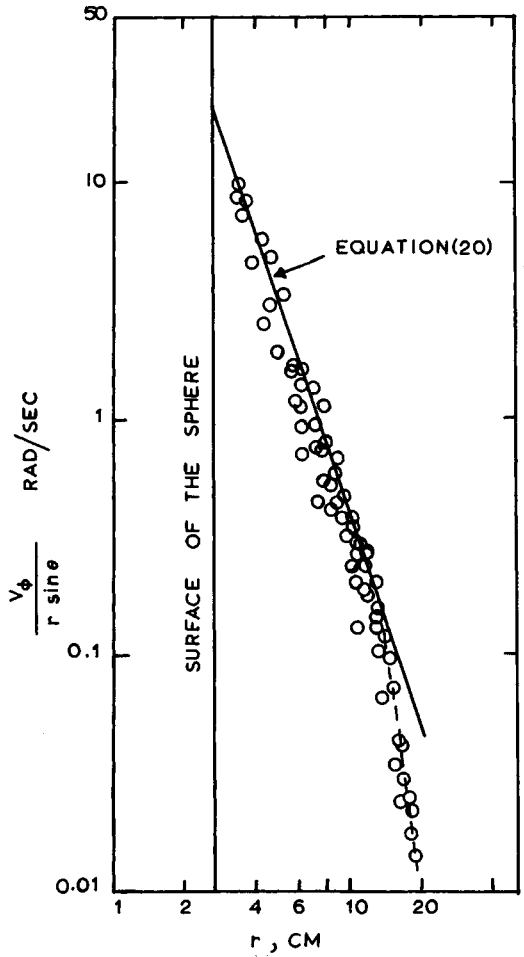

Fig. 3. Primary velocity distribution for a sphere rotating in a Newtonian glycerol solution compared with the theoretical result (rpm = 200).

ences as well. For instance, at a shear rate of 10 sec^{-1}, it showed shear stress of 180 $dyne/cm^2$, whereas the primary normal stress difference was 500 $dyne/cm^2$.

A qualitative observation of the flow patterns in such a solution was made when the sphere was rotated at 50 rpm and 200 rpm. It was found that although the secondary flow was generated because of the presence of inertia as well as elasticity, the influence of elasticity was far more dominating. Thus, the entire flow field in the fluid was completely reversed. In the experiments with the Newtonian liquids at the same rotational speeds the liquid was drawn from the poles and thrown away near the equator. In the case of this viscoelastic liquid, however, the fluid was drawn in near the equator and thrown away at the poles. The secondary flows observed in Newtonian and viscoelastic liquids are shown qualitatively in Figure 4.

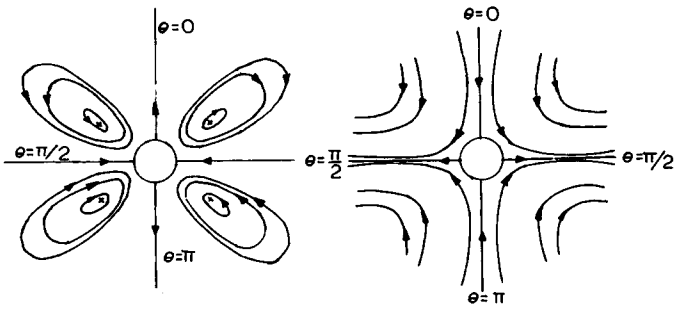

Fig. 4. Secondary flow in (a) viscoelastic liquid and (b) Newtonian liquid.

The influence of such a strong secondary flow due to inertia and elasticity on the primary velocity distribution is now examined. The theoretical expression used for comparison was that approximated by equation (16). This expression may be rewritten as,

$$\frac{v_\phi}{r \sin \theta} = \Omega a^{3/n} r^{-3/n} \tag{22}$$

Once again a plot of $v_\phi/(r \sin \theta)$ versus r on a log–log scale should give the slope as $-3/n$ and also satisfy the boundary condition $v_\phi = r\Omega \sin \theta$ at $r = a$. Figures 5 and 6 show the comparison between the theoretical and experimental values. Inspite of the presence of strong secondary velocities, the data appear to be very well approximated by the expression (22).

The corresponding velocity distribution for a Newtonian liquid is also shown. The previous theoretical analyses[4,5] predict little or no departure of the primary velocity distribution from the Newtonian velocity distribution. The divergence of the experimental velocity distributions from this line clearly points out the inadequacy of the theoretical analyses, which has been emphasized earlier. It is interesting further to see that the wall effects observed in the previous case were not detected in this case. This is perhaps due to the strong shear dependence of viscosity (low value of n). Equation (22) shows that $v_\phi/(r\Omega \sin \theta)$ is reduced much more rapidly than in the case of a Newtonian liquid. This damping effect is perhaps responsible for the sound agreement near the wall.

These favorable comparisons for the velocity distributions give some encouragement for examining the torque-angular velocity data in the light of eq. (18). Rearranging this equation as

$$\log (T/a^3) = \log \left\{ 4\pi K (3/n)^n \int_0^{\pi/2} (\sin \theta)^{2+n} \, d\theta \right\} + n \log \Omega \tag{23}$$

indicates that a plot of $\log (T/a^3)$ versus $\log \Omega$ gives n as the slope, and the consistency index K could be obtained from the intercept. Figure 7 shows one such typical plot for a polyacrylamide solution (1%). The data were obtained by rotating three spheres of radii 0.635, 1.27, and 1.765

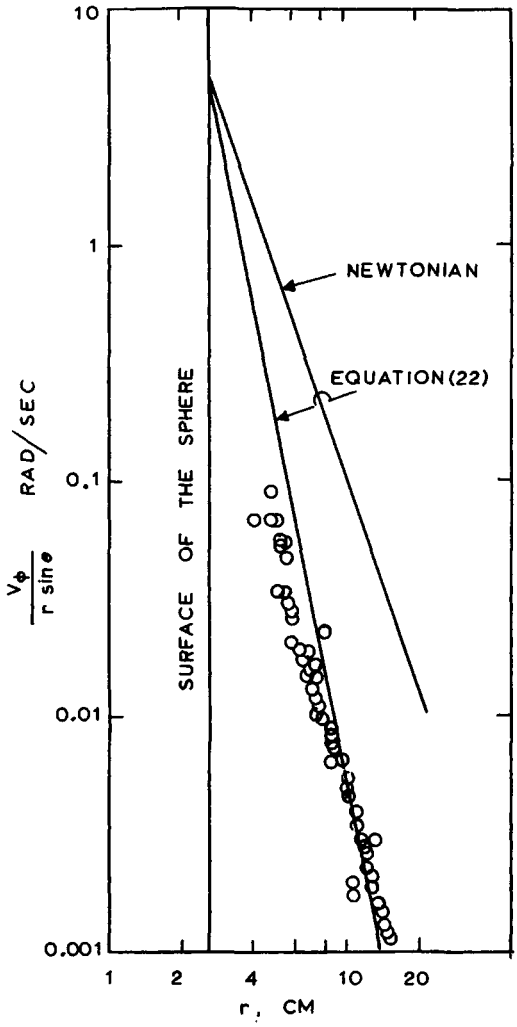

Fig. 5. Primary velocity distribution for a sphere rotating in a viscoelastic PAA–HEC solution compared with the theoretical result (rpm = 50).

cm, respectively. A good straight line is obtained. The values of K = 44.7 and n = 0.38 obtained from such a plot compare very favorably with those obtained from a Weissenberg rheogoniometer, which were K = 45.2 and n = 0.37. The CMC solution used in this work did not show any measurable normal stress differences and was considered to be inelastic as compared to PAA solutions, which were strongly viscoelastic. Table I shows a comparison between the values of K and n obtained from a rotating sphere viscometer and the Weissenberg rheogoniometer. A satisfactory agreement is found in all the cases.

These results appear to be encouraging and establish a rotating sphere viscometer as a useful tool for the measurement of the parameters in the

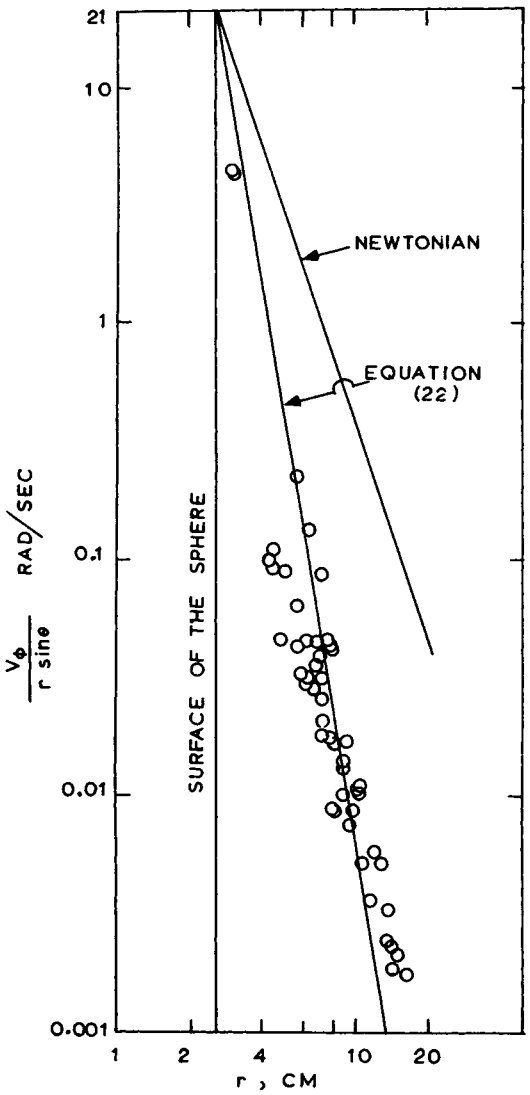

Fig. 6. Primary velocity distribution for a sphere rotating in a viscoelastic PAA–HEC solution compared with the theoretical result (rpm = 200).

flow curve. A further discussion of the use of such a viscometer is in order. The following points need to be considered in this respect:

1. In order to avoid wall effects, a sufficiently large ratio of the vessel diameter to the sphere diameter will have to be maintained. This will necessitate a rather large volume of liquid (up to 20 liters). This is a clear disadvantage when only small samples are available. As shown in this work, however, ratio of vessel diameter to sphere diameter as low as 5 could be kept, which could reduce the sample requirement considerably.

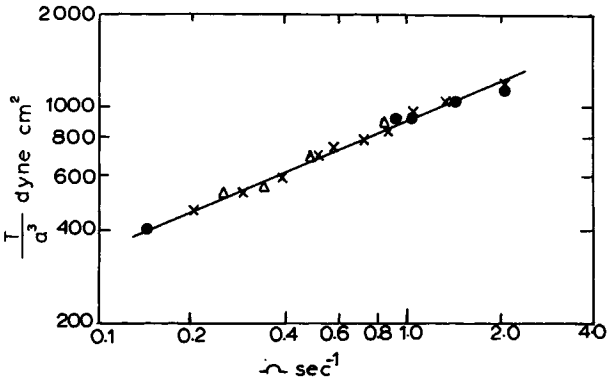

Fig. 7. Experimental plot of log (T/a^3) vs. log Ω for 1% PAA solution obtained on a RSV: (X) 2.64-cm-diam. sphere; (●) 1.765-cm-diam. sphere; (Δ) 1.27-cm-diam. sphere.

2. The analysis in this work shows how to obtain the parameters in the equation describing the flow curve but does not show how to obtain a mean shear stress–shear rate curve. This means that the equation chosen for describing the flow curve must be adequate in the range of average shear rates encountered in the rotating sphere viscometer. Due to the local variation in shear rates, it is difficult to ascribe an exact value of a representative shear rate. However, since the flow curves can generally be correlated satisfactorily over at least two to three orders of magnitude of shear rates, even an approximate order of magnitude estimate may be useful. For this reason, a pseudo-Newtonian average shear rate[1] of $3\pi/4\Omega$ may be used as a rough estimation of average shear rate at each Ω.

3. The viscometer can be used for both inelastic and viscoelastic liquids but its use is recommended only at moderate Reynolds numbers ($Re \leq 5$). This is not too severe a restriction provided the test liquids are sufficiently viscous, which is anyway the case with most polymer solutions of reasonably high concentrations and polymer melts.

TABLE I
Comparison of the Parameters of Ostwald-de Waele Model Obtained from Weissenberg Rheogoniometer and Rotating Sphere

	K, $\frac{\text{dyne sec}^n}{\text{cm}^2}$		n	
Solution used	Weissenberg	Rotating sphere	Weissenberg	Rotating sphere
1% CMC (inelastic)	50	47.6	0.63	0.59
1% PAA (viscoelastic)	45.2	44.7	0.37	0.38
2% PAA (viscoelastic)	133.3	130.7	0.31	0.32

References

1. R. A. Mashelkar, D. D. Kale, J. V. Kelkar, and J. Ulbrecht, *Chem. Eng. Sci.*, **27**, 973 (1972).
2. K. Wichterle and J. Ulbrecht, *Rheol. Acta*, **4**, 299 (1967).
3. D. D. Kale, R. A. Mashelkar, and J. Ulbrecht, *Nature* (Phy. Sci.), **242**, 29 (1973).
4. H. Giesekus, *Proc. 4th Int. Congress Rheology (Providence)*, **1**, 249 (1965).
5. K. Walters and J. G. Savins, *Trans. Soc. Rheol.*, **9**, 407 (1965).
6. R. A. Hermes, *J. Appl. Polym. Sci.*, **10**, 1793 (1966).
7. H. Lamb, *Hydrodynamics*, 5th ed., Cambridge University Press, Cambridge, 1924, p. 557.
8. R. H. Thomas and K. Walters, *Quart. J. Mech. Appl. Math.*, **17**, 39 (1964).
9. S. Middleman, *The Flow of High Polymers*, Interscience, New York, 1968.
10. J. V. Kelkar, Ph.D. Thesis, University of Salford, England, 1972.
11. R. B. Bird, W. E. Stewart, and E. N. Lightfoot, *Transport Phenomena*, Wiley, New York, 1960.

Received October 23, 1972